

# $B^0 - \overline{B^0}$ mixing, $B \rightarrow J/\psi K_s$ and $B \rightarrow X_d \gamma$ in general MSSM

P. Ko and Jae-hyeon Park

*Department of Physics, KAIST  
Daejeon 305-701, Korea*

G. Kramer

*II. Institut für Theoretische Physik,  
Universität Hamburg  
D-22761 Hamburg, Germany*  
(Dated: November 1, 2018)

## Abstract

We consider the gluino-mediated SUSY contributions to  $B^0 - \overline{B^0}$  mixing,  $B \rightarrow J/\psi K_s$  and  $B \rightarrow X_d \gamma$  in the mass insertion approximation. We find the ( $LL$ ) mixing parameter can be as large as  $|(\delta_{13}^d)_{LL}| \lesssim 2 \times 10^{-1}$ , but the ( $LR$ ) mixing is strongly constrained by the  $B \rightarrow X_d \gamma$  branching ratio and we find  $|(\delta_{13}^d)_{LR}| \lesssim 10^{-2}$ . The implications for the direct CP asymmetry in  $B \rightarrow X_d \gamma$  and the dilepton charge asymmetry ( $A_{ll}$ ) are also discussed, where substantial deviations from the standard model (SM) predictions are possible.

## I. INTRODUCTION

Recent observations of large CP violation in  $B \rightarrow J/\psi K_s$  [1, 2] giving

$$\sin 2\beta = (0.79 \pm 0.10) \quad (1)$$

confirm the SM prediction and begin to put a strong constraint on new physics contributions to  $B^0 - \overline{B^0}$  mixing and  $B \rightarrow J/\psi K_s$ , when combined with  $\Delta m_{B_d} = (0.472 \pm 0.017) \text{ ps}^{-1}$  [3]. Since the decay  $B \rightarrow J/\psi K_s$  is dominated by the tree level SM process  $b \rightarrow c\bar{c}s$ , we expect the new physics contribution may affect significantly only the  $B^0 - \overline{B^0}$  mixing and not the decay  $B \rightarrow J/\psi K_s$ . A model independent study of  $B^0 - \overline{B^0}$  mixing has been discussed recently by Laplace et al. [4]. However, in the presence of new physics contributions to  $B^0 - \overline{B^0}$  mixing, the same new physics would generically affect the  $B \rightarrow X_d\gamma$  process. The relation between the new physics effects on the  $B^0 - \overline{B^0}$  mixing and  $B \rightarrow X_d\gamma$  is in principle independent of each other and one may adopt a model independent analysis based on effective lagrangian with dimension 5 or 6 operators (for example, see Ref. [5] for the model independent study of the correlation between  $B \rightarrow X_s\gamma$  and  $B \rightarrow X_s l^+ l^-$ . The second paper in Ref. [5] includes a new CP violating phase in the  $C_{7\gamma}$  Wilson coefficient.). This approach would introduce 4 new independent complex parameters: two in the  $B^0 - \overline{B^0}$  mixing, and two in the  $B \rightarrow X_d\gamma$ . Being with too many independent parameters, one would not be able to get definite predictions based on this approach.

In this work, we do not attempt a completely model independent study with too many new independent parameters. Instead, we consider  $B^0 - \overline{B^0}$  mixing,  $B \rightarrow J/\psi K_s$  and  $B_d \rightarrow X_d\gamma$  in general SUSY models where flavor and CP violation due to the gluino mediation can be important. The chargino-stop and the charged Higgs-top loop contributions are parametrically suppressed relative to the gluino contributions, and thus ignored following Ref. [6]. (See however Refs. [7, 8] for including such effects. Another popular approach which is orthogonal to our approach is the minimal flavor violation model, which is discussed in Refs. [9] in the context of  $B$  physics.) We use the mass insertion approximation (MIA) for this purpose. Comprehensive work has been done for the first two observables in the MIA considering  $\Delta m_{B_d}$  and  $\sin 2\beta$  constraints only (see Ref. [2] for the most recent studies with such an approach). In our work, we also include the dilepton charge asymmetry  $A_{ll}$  and the  $B_d \rightarrow X_d\gamma$  branching ratio constraint extracted from the recent experimental upper limit on the  $B \rightarrow \rho\gamma$  branching ratio [10]

$$B(B \rightarrow \rho\gamma) < 2.3 \times 10^{-6},$$

and rederive the upper limits on the  $(\delta_{13}^d)_{LL}$  and  $(\delta_{13}^d)_{LR}$  mixing parameters assuming that only one of these gives a dominant SUSY contribution in addition to the standard model (SM) contribution. In addition we study the direct CP asymmetry in  $B_d \rightarrow X_d\gamma$  on the basis of our result for the SUSY contribution, and discuss how much deviations from the SM predictions are expected. Although we confine ourselves here to the gluino-mediated SUSY contributions only, our strategy can be extended to any new physics scenario with a substantial contribution to  $B^0 - \overline{B^0}$  mixing and  $B \rightarrow X_d\gamma$ .

## II. EFFECTIVE HAMILTONIANS FOR $B^0 - \overline{B^0}$ MIXING AND $B \rightarrow X_d \gamma$

### A. Effective Hamiltonian for $B^0 - \overline{B^0}$ mixing

The most general effective Hamiltonian for  $B^0 - \overline{B^0}$  mixing ( $\Delta B = 2$ ) can be written in the following form [2]:

$$H_{\text{eff}}^{\Delta B=2} = \sum_{i=1}^5 C_i Q_i + \sum_{i=1}^3 \tilde{C}_i \tilde{Q}_i, \quad (2)$$

where the operators  $Q_i$ 's are defined as

$$\begin{aligned} Q_1 &= \bar{d}_L^\alpha \gamma_\mu b_L^\alpha \bar{d}_L^\beta \gamma^\mu b_L^\beta \\ Q_2 &= \bar{d}_R^\alpha b_L^\alpha \bar{d}_R^\beta b_L^\beta \\ Q_3 &= \bar{d}_R^\alpha b_L^\beta \bar{d}_R^\beta b_L^\alpha \\ Q_4 &= \bar{d}_R^\alpha b_L^\alpha \bar{d}_L^\beta b_R^\beta \\ Q_5 &= \bar{d}_R^\alpha b_L^\beta \bar{d}_L^\beta b_R^\alpha \end{aligned} \quad (3)$$

and the operators  $\tilde{Q}_i$  are obtained from  $Q_i$ 's by the exchange of  $L \leftrightarrow R$ .  $\alpha, \beta$  are color indices, and  $q_{L,R} \equiv (1 \mp \gamma_5)q/2$ . The Wilson coefficients  $C_i$ 's receive contributions from both the SM and the SUSY loops:  $C_i \equiv C_i^{\text{SM}} + C_i^{\text{SUSY}}$ .

In the SM, the  $t - W$  box diagram generates only contribution to the operator  $Q_1$ , and the corresponding Wilson coefficient  $C_1^{\text{SM}}$  at the  $m_t$  scale is given by [11]

$$C_1^{\text{SM}}(m_t) = \frac{G_F^2}{4\pi^2} M_W^2 (V_{td}^* V_{tb})^2 S_0(x_t), \quad (4)$$

where

$$S_0(x_t) = \frac{4x_t - 11x_t^2 + x_t^3}{4(1 - x_t)^2} - \frac{3x_t^3 \ln x_t}{2(1 - x_t)^3}, \quad (5)$$

with  $x_t \equiv m_t^2/m_W^2$ . Performing the RG evolution down to  $m_b$  scale incorporating the NLO QCD corrections [12], we get  $C_1^{\text{SM}}$  at  $m_b$ :

$$C_1^{\text{SM}}(m_b) = \frac{G_F^2}{4\pi^2} M_W^2 (V_{td}^* V_{tb})^2 \eta_{2B} S_0(x_t) [\alpha_s(m_b)]^{-6/23} \left[ 1 + \frac{\alpha_s(m_b)}{4\pi} J_5 \right]. \quad (6)$$

The definition of  $J_5$  can be found in Ref. [13], and we use the value of the QCD correction factor  $\eta_{2B} = 0.551$  therein. Evaluating the matrix element of  $Q_1$ , we set the bag parameter  $B_1(m_b)$  in the  $\overline{\text{MS}}(\text{NDR})$  scheme to 0.87 [14], which is numerically equal to the value in the RI-MOM scheme in Eqs. (12).

If the deviation of the squark mass matrix from universality is small, the SUSY contribution from the gluino-squark loop is best studied in the mass insertion approximation, which renders the flavor structures of the processes manifest. Flavor violations in the squark sector are parameterized by sizes of the off-diagonal mass matrix elements relative to the average squared squark mass,

$$(\delta_{ij}^d)_{AB} \equiv (\tilde{m}_{ij}^d)_{AB} / \tilde{m}^2, \quad (7)$$

where  $i$  and  $j$  are family indices and  $A$  and  $B$  are chiralities,  $L$  or  $R$ . The mass matrix is understood to be in the super-CKM basis so that the quark-squark-gluino interaction vertex preserves flavor. This method is applicable to a model-independent study of flavor and/or CP violation in the squark sector when the series expansion in terms of  $(\delta_{ij}^d)_{AB}$  is meaningful. In the presence of general (but small) flavor mixings in the down-type squark mass matrix, the squark-gluino box diagrams give the Wilson coefficients [6],

$$\begin{aligned}
C_1^{\text{SUSY}} &= -\frac{\alpha_s^2}{216\tilde{m}^2} \left( 24xf_6(x) + 66\tilde{f}_6(x) \right) (\delta_{13}^d)_{LL}^2 \\
C_2^{\text{SUSY}} &= -\frac{\alpha_s^2}{216\tilde{m}^2} 204xf_6(x) (\delta_{13}^d)_{RL}^2 \\
C_3^{\text{SUSY}} &= \frac{\alpha_s^2}{216\tilde{m}^2} 36xf_6(x) (\delta_{13}^d)_{RL}^2 \\
C_4^{\text{SUSY}} &= -\frac{\alpha_s^2}{216\tilde{m}^2} \left[ \left( 504xf_6(x) - 72\tilde{f}_6(x) \right) (\delta_{13}^d)_{LL} (\delta_{13}^d)_{RR} \right. \\
&\quad \left. - 132\tilde{f}_6(x) (\delta_{13}^d)_{LR} (\delta_{13}^d)_{RL} \right] \\
C_5^{\text{SUSY}} &= -\frac{\alpha_s^2}{216\tilde{m}^2} \left[ \left( 24xf_6(x) + 120\tilde{f}_6(x) \right) (\delta_{13}^d)_{LL} (\delta_{13}^d)_{RR} \right. \\
&\quad \left. - 180\tilde{f}_6(x) (\delta_{13}^d)_{LR} (\delta_{13}^d)_{RL} \right]. \tag{8}
\end{aligned}$$

The other Wilson coefficients  $\tilde{C}_{i=1,2,3}^{\text{SUSY}}$ 's are obtained from  $C_{i=1,2,3}^{\text{SUSY}}$  by exchange of  $L \leftrightarrow R$ . The loop functions  $f_6(x)$  and  $\tilde{f}_6(x)$ , evaluated in terms of  $x \equiv m_{\tilde{g}}^2/\tilde{m}^2$ , are given by

$$\begin{aligned}
f_6(x) &= \frac{6(1+3x)\ln x + x^3 - 9x^2 - 9x + 17}{6(x-1)^5}, \\
\tilde{f}_6(x) &= \frac{6x(1+x)\ln x - x^3 - 9x^2 + 9x + 1}{3(x-1)^5}. \tag{9}
\end{aligned}$$

These Wilson coefficients are calculated at  $\mu \sim m_{\tilde{g}} \sim \tilde{m}$ , and evolved down to the  $m_b$  scale. A complete NLO RG evolution formula of these Wilson coefficients is available in Ref. [2]. The initial condition (8) is at LO in  $\alpha_s$ , but it would be no problem to include the NLO correction. For this we use

$$C_r(m_b^{pole}) = \sum_i \sum_s \left( b_i^{(r,s)} + \eta c_i^{(r,s)} \right) \eta^{a_i} C_s(M_S), \tag{10}$$

where the SUSY scale is defined by  $M_S = (\tilde{m} + m_{\tilde{g}})/2$ , and  $\eta = \alpha_s(M_S)/\alpha_s(m_t)$ . The list of ‘magic numbers’  $a_i$ ,  $b_i^{(r,s)}$ , and  $c_i^{(r,s)}$ , in the RI-MOM scheme, can be found in Ref. [2]. RG running of  $\tilde{C}_{1-3}$  is done in the same way as for  $C_{1-3}$ .

Each matrix element of the  $\Delta B = 2$  operators in (3) is taken to be a product of its value

in vacuum insertion approximation and the corresponding bag parameter:

$$\begin{aligned}
\langle B_d | Q_1(\mu) | \overline{B^0} \rangle &= \frac{2}{3} m_{B_d}^2 f_{B_d}^2 B_1(\mu), \\
\langle B_d | Q_2(\mu) | \overline{B^0} \rangle &= -\frac{5}{12} \left( \frac{m_{B_d}}{m_b(\mu) + m_d(\mu)} \right)^2 m_{B_d}^2 f_{B_d}^2 B_2(\mu), \\
\langle B_d | Q_3(\mu) | \overline{B^0} \rangle &= \frac{1}{12} \left( \frac{m_{B_d}}{m_b(\mu) + m_d(\mu)} \right)^2 m_{B_d}^2 f_{B_d}^2 B_1(\mu), \\
\langle B_d | Q_4(\mu) | \overline{B^0} \rangle &= \frac{1}{2} \left( \frac{m_{B_d}}{m_b(\mu) + m_d(\mu)} \right)^2 m_{B_d}^2 f_{B_d}^2 B_1(\mu), \\
\langle B_d | Q_5(\mu) | \overline{B^0} \rangle &= \frac{1}{6} \left( \frac{m_{B_d}}{m_b(\mu) + m_d(\mu)} \right)^2 m_{B_d}^2 f_{B_d}^2 B_1(\mu).
\end{aligned} \tag{11}$$

Here we use the lattice improved calculations for the bag parameters in the RI-MOM scheme [14]:

$$\begin{aligned}
B_1(m_b) &= 0.87(4)^{+5}_{-4}, & B_2(m_b) &= 0.82(3)(4), \\
B_3(m_b) &= 1.02(6)(9), & B_4(m_b) &= 1.16(3)^{+5}_{-7}, \\
B_5(m_b) &= 1.91(4)^{+22}_{-7}.
\end{aligned} \tag{12}$$

In addition, we use the following running quark masses in the RI-MOM scheme :

$$m_b(m_b) = 4.6 \text{ GeV}, \quad m_d(m_b) = 5.4 \text{ MeV}. \tag{13}$$

The bottom quark mass is obtained from the  $\overline{MS}$  mass  $m_b^{\overline{MS}}(m_b^{\overline{MS}}) = 4.23$  GeV. For the  $B_d$  meson decay constant, we assume  $f_{B_d} = 200 \pm 30$  MeV.

The above  $\Delta B = 2$  effective Hamiltonian will contribute to  $\Delta m_B$ , the dilepton charge asymmetry and the time dependent CP asymmetry in the decay  $B \rightarrow J/\psi K_s$  via the phase of the  $B^0 - \overline{B^0}$  mixing. Defining the mixing matrix element by

$$M_{12}(B^0) \equiv \frac{1}{2m_B} \langle B^0 | H_{\text{eff}}^{\Delta B=2} | \overline{B^0} \rangle \tag{14}$$

one has  $\Delta m_{B_d} = 2|M_{12}(B_d^0)|$ . This quantity is dominated by the short distance contributions, unlike the  $\Delta m_K$  for which long distance contributions would be significant. Therefore the data on  $\Delta m_{B_d}^{\text{exp}}$  will constrain the modulus of  $M_{12}(B_d^0)$ . On the other hand, the phase of the  $B^0 - \overline{B^0}$  mixing amplitude  $M_{12}(B^0) \equiv \exp(2i\beta') |M_{12}(B^0)|$  appears in the time dependent asymmetry :

$$A_{\text{CP}}^{\text{mix}}(B^0 \rightarrow J/\psi K_s) = \sin 2\beta' \sin \Delta m_{B_d} t. \tag{15}$$

Since there may be large new physics (SUSY in this work) contributions to both  $K^0 - \overline{K^0}$  and  $B^0 - \overline{B^0}$  mixings, the CKM fit may change accordingly. Only those constraints that come from semileptonic processes may be used, since these will be dominated by the SM contributions at tree level (unless one considers R-parity violation). Therefore the angle  $\beta'$  need not be the same as the SM angle  $\beta (= \phi_1)$ , and the angle  $\gamma (= \phi_3)$  should be considered as a free parameter in the full range from 0 to  $2\pi$  in principle. This strategy was also adopted in some earlier work [2, 15].

TABLE I: Input values for the parameters.

$m_{B_d}$	5.279 GeV
$m_t$	174 GeV
$ V_{cb} $	$(40.7 \pm 1.9) \times 10^{-3}$
$ V_{ub} $	$(3.61 \pm 0.46) \times 10^{-3}$
$f_{B_d}$	$200 \pm 30$ MeV
$\alpha_s(M_Z)$	0.119

Finally, the dilepton charge asymmetry  $A_{ll}$  is also determined by  $M_{12}(B^0)$ , albeit a possible long distance contribution to  $\Gamma_{SM}(B^0)$ . Defining the mass eigenstates of the neutral  $B^0$  mesons as

$$|B_{1,2}\rangle \equiv \frac{1}{\sqrt{1+|\eta|^2}} \left[ |B^0\rangle \pm \eta |\overline{B^0}\rangle \right],$$

with  $\eta \equiv \sqrt{(M_{12}^* - i\Gamma_{12}^*)/(M_{12} - i\Gamma_{12})}$ , we can derive the following relation:

$$A_{ll} \equiv \frac{N(BB) - N(\bar{B}\bar{B})}{N(BB) + N(\bar{B}\bar{B})} = -\frac{|\eta|^4 - 1}{|\eta|^4 + 1} = \frac{\text{Im}(\Gamma_{12}/M_{12})}{1 + |\Gamma_{12}/M_{12}|^2/4} \approx \text{Im}(\Gamma_{12}/M_{12}). \quad (16)$$

Here  $M_{12}, \Gamma_{12}$  are the matrix elements of the Hamiltonian in the  $(B^0, \overline{B^0})$  basis:

$$\frac{1}{2m_B} \langle \overline{B} | H_{\text{full}} | B \rangle = M_{12} - \frac{i}{2} \Gamma_{12}.$$

In the SM, the phases of  $M_{12}$  and  $\Gamma_{12}$  are approximately equal and

$$\Delta M_{\text{SM}} \approx 2|M_{12}^{\text{SM}}|, \quad \Delta \Gamma_{\text{SM}} \approx 2|\Gamma_{12}^{\text{SM}}|.$$

the quantity  $\Gamma_{12}^{\text{SM}}$  is given by [16]

$$\begin{aligned} \Gamma_{12}^{\text{SM}} = & (-1) \frac{G_F^2 m_b^2 M_{B_d} B_{B_d} f_{B_d}^2}{8\pi} \left[ v_t^2 + \frac{8}{3} v_c v_t \left( z_c + \frac{1}{4} z_c^2 - \frac{1}{2} z_c^3 \right) + \right. \\ & \left. v_c^2 \left\{ \sqrt{1-4z_c} \left( 1 - \frac{2}{3} z_c \right) + \frac{8}{3} z_c + \frac{2}{3} z_c^2 - \frac{4}{3} z_c^3 - 1 \right\} \right], \end{aligned} \quad (17)$$

where  $v_i \equiv V_{ib} V_{id}^*$  and  $z_c \equiv m_c^2/m_b^2$ . Varying  $f_{B_d}$ ,  $|V_{ub}|$ , and  $|V_{cb}|$  in the range quoted in Table I, and  $\gamma$  inside the range given by  $(54.8 \pm 6.2)^\circ$  [17], we get the SM value to be

$$-1.54 \times 10^{-3} \leq A_{ll}^{\text{SM}} \leq -0.16 \times 10^{-3},$$

whereas the current world average is [4]

$$A_{ll}^{\text{exp}} \approx (0.2 \pm 1.4) \times 10^{-2}.$$

In the presence of SUSY, the phases of  $M_{12}$  and  $\Gamma_{12}$  may be no longer the same, and potentially a larger dilepton charge asymmetry may be possible. In particular,  $M_{12}$  could be affected strongly by SUSY particles, whereas  $\Gamma_{12}$  is not, i.e.  $M_{12}^{\text{FULL}} = M_{12}^{\text{SM}} + M_{12}^{\text{SUSY}}$  whereas  $\Gamma_{12}^{\text{FULL}} \approx \Gamma_{12}^{\text{SM}}$ . In this case, the dilepton charge asymmetry could be approximated as

$$A_{ll} = \text{Im} \left( \frac{\Gamma_{12}^{\text{SM}}}{M_{12}^{\text{SM}} + M_{12}^{\text{SUSY}}} \right). \quad (18)$$

The possible ranges of  $A_{ll}$  in a class of general SUSY models were studied in Ref. [18].

## B. Effective Hamiltonian for $\Delta B = 1$ processes

The effective Hamiltonian relevant to  $\Delta B = 1$  processes involves four quark operators and  $b \rightarrow d\gamma$  and  $b \rightarrow dg$  penguin operators. Since we are not going to discuss  $\Delta B = 1$  nonleptonic decays due to theoretical uncertainties related with factorization, we shall consider the inclusive radiative decay  $B \rightarrow X_d\gamma$  only. The relevant effective Hamiltonian for this process is given by [19]

$$\begin{aligned} \mathcal{H}_{\text{eff}}(b \rightarrow d\gamma(+g)) = & -\frac{4G_F}{\sqrt{2}} V_{td}^* V_{tb} \sum_{i=1,2,7,8} C_i(\mu_b) O_{ic}(\mu_b) \\ & + \frac{4G_F}{\sqrt{2}} V_{ud}^* V_{ub} \sum_{i=1,2} C_i(\mu_b) [O_{iu}(\mu_b) - O_{ic}(\mu_b)] \end{aligned} \quad (19)$$

with

$$\begin{aligned} O_{1c} &= \bar{d}_L \gamma^\mu c_L \bar{c}_L \gamma_\mu b_L, & O_{1u} &= \bar{d}_L \gamma^\mu u_L \bar{u}_L \gamma_\mu b_L, \\ O_{2c} &= \bar{d}_L \gamma^\mu c_L \bar{c}_L \gamma_\mu b_L, & O_{2u} &= \bar{d}_L \gamma^\mu u_L \bar{u}_L \gamma_\mu b_L, \\ O_{7\gamma} &= \frac{e}{16\pi^2} m_b \bar{d}_L \sigma^{\mu\nu} F_{\mu\nu} b_R, & O_{8g} &= \frac{g_s}{16\pi^2} m_b \bar{d}_L \sigma^{\mu\nu} t^a G_{\mu\nu}^a b_R. \end{aligned} \quad (20)$$

Here the renormalization scale  $\mu_b$  is of the order of  $m_b$ , and we have used the unitarity of the CKM matrix elements

$$V_{cd}^* V_{cb} = -(V_{ud}^* V_{ub} + V_{td}^* V_{tb}),$$

which should be valid even in the presence of SUSY flavor violations.

In the SM, all the three up-type quarks contribute to this decay, since all the relevant CKM factors are of the same order of magnitude. The strong phases are provided by the imaginary parts of one loop diagrams at the order  $O(\alpha_s)$  by the usual unitarity argument. Varying  $f_{B_d}$ ,  $|V_{ub}|$ , and  $|V_{cb}|$  in the range quoted in Table I, and  $\gamma$  between  $(54.8 \pm 6.2)^\circ$  [17], we get the branching ratio for this decay in the SM to be  $8.9 \times 10^{-6} - 1.1 \times 10^{-5}$ . The direct CP asymmetry in the SM is about  $-15\% - -10\%$  [19]. We have updated the previous predictions by Ali et al. [19] using the present values of CKM parameters.

The CP averaged branching ratio for  $B \rightarrow X_d\gamma$  in the leading log approximation is given by [19, 20, 21]

$$\frac{B(B \rightarrow X_d\gamma)}{B(B \rightarrow X_c e \bar{\nu})} = \left| \frac{V_{td}^* V_{tb}}{V_{cb}} \right|^2 \frac{6\alpha}{\pi f(z)} |C_7(m_b)|^2. \quad (21)$$

where  $f(z) = 1 - 8z + 8z^3 - z^4 - 12z^2 \ln z$  is the phase space factor for the  $b \rightarrow c$  semileptonic decays and  $\alpha^{-1} = 137.036$ . Neglecting the RG running between the heavy SUSY particles and the top quark mass scale, we get the following relations :

$$\begin{aligned} C_7(m_b) &\approx -0.31 + 0.67 C_7^{\text{new}}(m_W) + 0.09 C_8^{\text{new}}(m_W), \\ C_8(m_b) &\approx -0.15 + 0.70 C_8^{\text{new}}(m_W). \end{aligned} \quad (22)$$

The new physics contributions to  $C_2$  are negligible so that we use  $C_2(m_b) = C_2^{\text{SM}}(m_b) \approx 1.11$ .

In general SUSY models considered in the present work, the Wilson coefficients  $C_{7\gamma}^{\text{new}}$  and  $C_{8g}^{\text{new}}$  are given by [8, 15, 22]

$$C_{7\gamma}^{\text{SUSY}}(m_W) = \frac{8\pi Q_b \alpha_s}{3\sqrt{2}G_F \tilde{m}^2 V_{td}^* V_{tb}} \left[ (\delta_{13}^d)_{LL} M_4(x) - (\delta_{13}^d)_{LR} \left( \frac{\tilde{m}\sqrt{x}}{m_b} \right) 4B_1(x) \right], \quad (23)$$

$$\begin{aligned} C_{8g}^{\text{SUSY}}(m_W) = & \frac{2\pi\alpha_s}{\sqrt{2}G_F \tilde{m}^2 V_{td}^* V_{tb}} \left[ (\delta_{13}^d)_{LL} \left( \frac{3}{2} M_3(x) - \frac{1}{6} M_4(x) \right) \right. \\ & \left. + (\delta_{13}^d)_{LR} \left( \frac{\tilde{m}\sqrt{x}}{m_b} \right) \frac{1}{6} (4B_1(x) - 9x^{-1}B_2(x)) \right] \end{aligned} \quad (24)$$

Here we have ignored the RG running between the squark and the gluino mass and the  $m_W$  scale. Note that the  $(\delta_{13}^d)_{LR}$  contribution is enhanced by  $m_{\tilde{g}}/m_b$  compared to the contributions from the SM and the  $LL$  insertion due to the chirality flip from the internal gluino propagator in the loop. Explicit expressions for the loop functions  $B_i$ 's and  $M_i$ 's can be found in Ref. [8, 15, 22].

In order to generate a nonvanishing direct CP asymmetry, one needs at least two independent amplitudes with different strong (CP-even) and weak (CP-odd) phases. In  $B \rightarrow X_d\gamma$ , strong phases are provided by quark and gluon loop diagrams, whereas weak phases are provided by the KM angles  $(\alpha, \beta, \gamma)$  and  $(\delta_{13}^d)_{AB}$ . The resulting direct CP asymmetry in  $B \rightarrow X_d\gamma$  can be written as [19, 20]

$$\begin{aligned} A_{\text{CP}}^{b \rightarrow d\gamma} (\text{in \%}) = & \frac{1}{|C_7|^2} [10.57 \text{ Im}(C_2 C_7^*) - 9.40 \text{ Im}((1 + \epsilon_d) C_2 C_7^*) \\ & - 9.51 \text{ Im}(C_8 C_7^*) + 0.12 \text{ Im}((1 + \epsilon_d) C_2 C_8^*)], \end{aligned} \quad (25)$$

where

$$\epsilon_d \equiv \frac{V_{ud}^* V_{ub}}{V_{td}^* V_{tb}} \approx \frac{(\rho - i\eta)}{(1 - \rho + i\eta)}$$

in the Wolfenstein parametrization for the CKM matrix elements.

A remark is in order for the above CP asymmetry in  $B \rightarrow X_d\gamma$ . Unlike the  $B \rightarrow X_s\gamma$  case for which the  $|C_{7\gamma}|$  is constrained by the observed  $B \rightarrow X_s\gamma$  branching ratio, the  $B \rightarrow X_d\gamma$  decay has not been observed yet, and its branching ratio can be vanishingly small even in the presence of new physics. In that case,  $|C_{7\gamma}| \approx 0$  so that the denominator of  $A_{\text{CP}}^{b \rightarrow d\gamma}$  becomes zero and the CP asymmetry blows up. This could be partly cured by replacing the denominator  $|C_{7\gamma}|^2$  by  $K_{\text{NLO}}(\delta)$  defined in Ref. [20]:

$$\begin{aligned} K_{\text{NLO}}(\delta) (\text{in \%}) = & 0.11 |C_2|^2 + 68.13 |C_7|^2 + 0.53 |C_8|^2 - 16.55 \text{ Re}(C_2 C_7^*) \\ & - 0.01 \text{ Re}(C_2 C_8^*) + 8.85 \text{ Re}(C_7 C_8^*) + 3.86 \text{ Re}(C_7^{(1)} C_7^*) \end{aligned} \quad (26)$$

for the photon energy cutoff factor  $\delta = 0.3$ . Here  $C_7^{(1)}$  is the next-to-leading order contribution to  $C_{7\gamma}(m_b)$  [20]:

$$C_{7\gamma}^{(1)} \approx 0.48 - 2.29 C_7^{\text{new}}(m_W) - 0.12 C_8^{\text{new}}(m_W). \quad (27)$$

This prescription will render the denominator of (25) to be finite.

### III. NUMERICAL ANALYSIS

In the numerical analysis, we impose the following quantities as constraints :

- $\Delta m_{B_d} = (0.472 \pm 0.017) \text{ ps}^{-1}$  : This constrains the modulus of  $M_{12}(B^0)$  through the following relation  $\Delta m_{B_d} = 2 |M_{12}(B^0)|$  [3].
- $A_{\text{CP}}^{\text{mix}} = (0.79 \pm 0.10)$  : This constrains the phase  $2\beta'$  of  $M_{12}(B^0)$  by  $A_{\text{CP}}^{\text{mix}} = \sin 2\beta'$ , where  $2\beta'$  is the argument of  $M_{12}(B^0)$  [4].
- $Br(B \rightarrow X_d\gamma) < 1 \times 10^{-5}$ : At present, there are limits only on the exclusive decays:  $B(B \rightarrow \rho\gamma) < 2.3 \times 10^{-6}$ . We assume a modest upper bound on the branching ratio for the inclusive radiative decay as  $Br(B \rightarrow X_d\gamma) \lesssim 1 \times 10^{-5}$ . This is also well below the experimental uncertainty in the  $B \rightarrow X_s\gamma$  branching ratio. This puts a strong constraint on both *LL* and *LR* insertions as we shall see. Especially the *LR* insertion is more strongly constrained, since its contribution is enhanced by  $m_{\tilde{g}}/m_b$  due to the chirality flip from the gluino in the loop compared to other contributions including the SM one. This is a new ingredient compared to the work in Ref. [2].
- $A_{ll}^{\text{exp}} = (0.2 \pm 1.4)\%$ : This is related to the  $B^0 - \overline{B^0}$  mixing through the relation (16). Although we do not use this constraint to restrict the allowed parameter space, we indicate the parameter space where the resulting  $A_{ll}$  falls out of the  $1\sigma$  range. It turns out that both *LL* and *LR* mixing scenarios are already strongly constrained by the  $B \rightarrow X_d\gamma$  branching ratio rather than by  $A_{ll}$ , as can be seen in Figs. 2 (a) and (b).

We impose these constraints at 68 % C.L. ( $1\sigma$ ) as we vary the KM angle  $\gamma$  between 0 and  $2\pi$ . In all cases, we set the common squark mass  $\tilde{m} = 500 \text{ GeV}$  and  $x = 1$  ( $m_{\tilde{g}} = \tilde{m}$ ). Finally for the mass insertion parameters  $(\delta_{13}^d)_{AB}$ , we consider two cases. In the first case (the *LL* case), only  $(\delta_{13}^d)_{LL}$  is nonvanishing among the mass insertion parameters, and in the second (the *LR* case), only  $(\delta_{13}^d)_{LR}$ . It would be straightforward to consider other possibilities such as  $(\delta_{13}^d)_{LL} = (\delta_{13}^d)_{RR}$  etc. in a similar way.

The parameter space searching is done in the following way. We vary  $\gamma$  from 0 to  $2\pi$ , and  $(\delta_{13}^d)_{AB}$  inside the bound depicted in Ref. [2]. For a given set of values of  $\gamma$  and  $(\delta_{13}^d)_{AB}$ , we search for those  $f_{B_d}$  and  $\sqrt{\rho^2 + \eta^2} \equiv |V_{ub}|/\lambda V_{cb}$  (with  $\lambda = |V_{us}|$ ) that satisfy  $1\sigma$  constraints on  $\Delta M_B$  and  $\sin 2\beta'$ . The search region is the  $1\sigma$  range in Table I. If no such pair exists, the  $(\gamma, (\delta_{13}^d)_{AB})$  point is excluded from the plots. Points that are not excluded are plotted in Fig. 1. Using these  $\gamma$ ,  $(\delta_{13}^d)_{AB}$ ,  $f_{B_d}$ , and  $\sqrt{\rho^2 + \eta^2}$  found above, we plot  $Br(B \rightarrow X_d\gamma)$  and  $A_{\text{CP}}^{B \rightarrow d\gamma}$ . Uncertainties in  $B_{1-3}(m_b)$ , which are actually used in our analysis, are only several per cent, while that in  $f_{B_d}$  is 15%. Moreover the matrix elements (11) are proportional to  $f_{B_d}^2 B_i(m_b)$ , so we do not take into account the uncertainties in the bag parameters.

In Figs. 1 (a) and (b), we show the allowed parameter space in the  $(\text{Re}(\delta_{13}^d)_{AB}, \text{Im}(\delta_{13}^d)_{AB})$  plane [(a) *LL* insertion and (b) *LR* insertion, respectively] for different values of the KM angle  $\gamma$  with different color codes: dark (red) for  $0^\circ \leq \gamma \leq 90^\circ$ , light gray (green) for  $90^\circ \leq \gamma \leq 180^\circ$ , very dark (blue) for  $180^\circ \leq \gamma \leq 270^\circ$  and gray (magenta) for  $270^\circ \leq \gamma \leq 360^\circ$ . The region leading to a too large branching ratio for  $B_d \rightarrow X_d\gamma$  is covered by slanted lines. And the region where  $A_{ll}$  falls out of the data within  $1\sigma$  range is already excluded by the  $B \rightarrow X_d\gamma$  branching ratio constraint. For both the *LL* and *LR* mixing cases, our results are the same as those in Ref. [2], if we impose only the  $\Delta m_{B_d}$  and  $\sin 2\beta$  constraints. By adding a constraint from  $B \rightarrow X_d\gamma$  (and  $A_{ll}$ ), the allowed parameter space is further reduced, and the

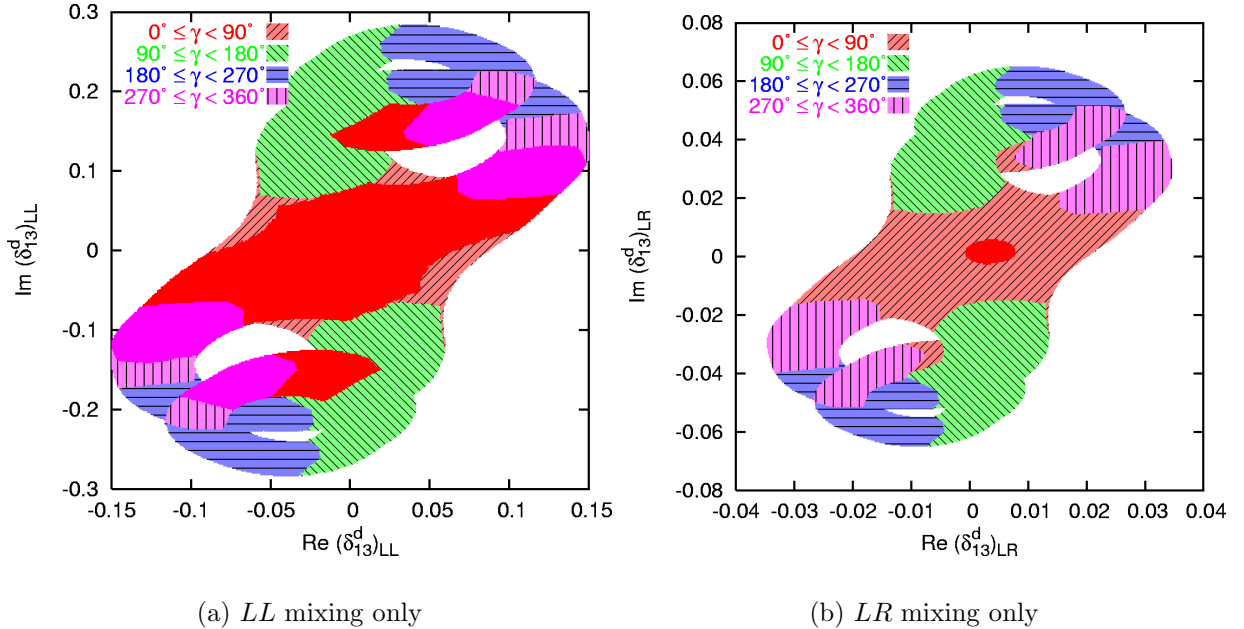


FIG. 1: The allowed ranges in (a) the  $LL$  and (b) the  $LR$  insertion cases for the parameters  $(\text{Re}(\delta_{13}^d)_{AB}, \text{Im}(\delta_{13}^d)_{AB})$  for different values of the KM angle  $\gamma$  with different color codes: dark (red) for  $0^\circ \leq \gamma \leq 90^\circ$ , light gray (green) for  $90^\circ \leq \gamma \leq 180^\circ$ , very dark (blue) for  $180^\circ \leq \gamma \leq 270^\circ$  and gray (magenta) for  $270^\circ \leq \gamma \leq 360^\circ$ . The region leading to a too large branching ratio for  $B_d \rightarrow X_d \gamma$  is colored lightly and covered by parallel lines.

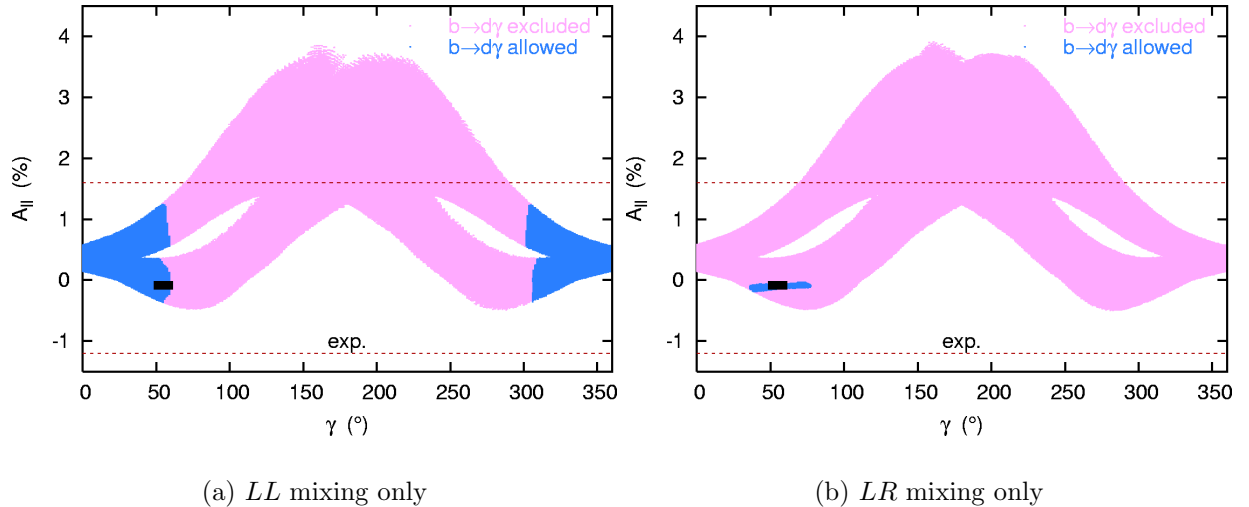


FIG. 2: The possible ranges of the dilepton charge asymmetry in (a) the  $LL$  and (b) the  $LR$  cases as functions of the KM angles  $\gamma$ . The black rectangle around  $\gamma \simeq 55^\circ$  is the SM prediction. Those parameters which lead to  $B(B \rightarrow X_d \gamma) > 1 \times 10^{-5}$  are denoted by the gray (magenta) region, and those for  $B(B \rightarrow X_d \gamma) < 1 \times 10^{-5}$  by the dark (blue) region. The  $1\sigma$  range for the world average of  $A_{ll}^{\text{exp.}} = (0.2 \pm 1.4)\%$  is shown to lie between the short dashed lines.

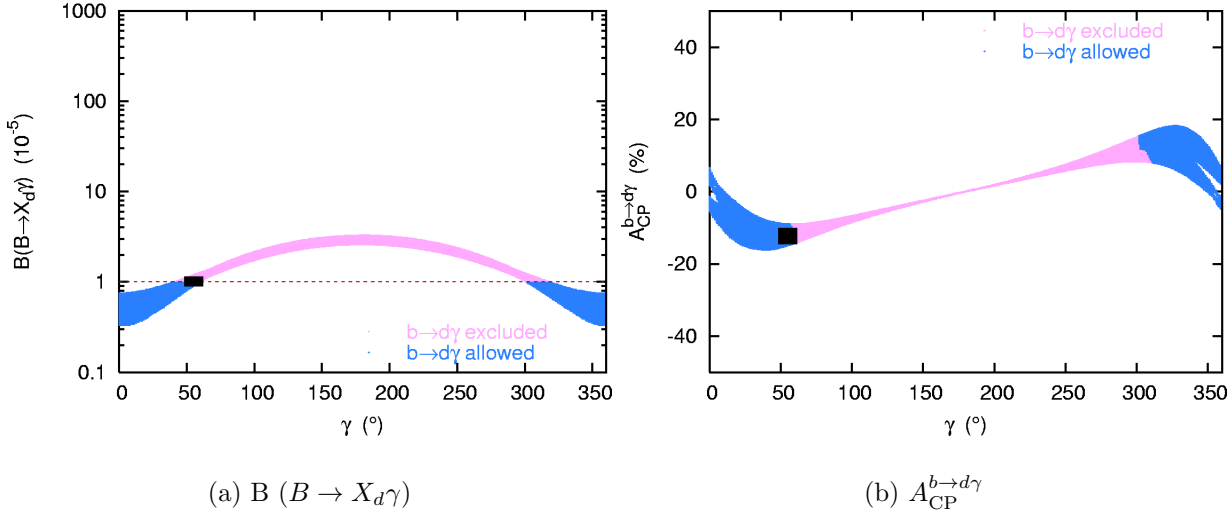


FIG. 3: The possible ranges of (a)  $B(B_d \rightarrow X_d \gamma)$  and (b)  $A_{CP}^{b \rightarrow d \gamma}$  as functions of the KM angle  $\gamma$  in the *LL* insertion case. The black rectangle around  $\gamma \simeq 55^\circ$  is the SM prediction. Those parameters which lead to  $B(B \rightarrow X_d \gamma) > 1 \times 10^{-5}$  are represented by the gray (magenta) region, and those for  $B(B \rightarrow X_d \gamma) < 1 \times 10^{-5}$  by the dark (blue) region.

effect is even larger for the *LR* mixing case. For the *LL* mixing [Fig. 1 (a)], the  $B \rightarrow X_d \gamma$  does play some role, and the  $A_{ll}$  gives a moderate constraint. The KM angle  $\gamma$  should be in the range between  $\sim -60^\circ$  and  $\sim +60^\circ$ , and  $A_{ll}$  can have the opposite sign compared to the SM prediction, even if the KM angle is the same as its SM value  $\gamma \simeq 55^\circ$ . For the *LR* mixing [Fig. 1 (b)], the  $B(B_d \rightarrow X_d \gamma)$  puts an even stronger constraint on the *LR* insertion, whereas the  $A_{ll}$  does not play any role. In particular, the KM angle  $\gamma$  can not be too much different from the SM value in the *LR* mixing case, once the  $B(B_d \rightarrow X_d \gamma)$  constraint is included. Only  $30^\circ \lesssim \gamma \lesssim 80^\circ$  is compatible with all the data from the  $B$  system, even if we do not consider the  $\epsilon_K$  constraint. The resulting parameter space is significantly reduced compared to the result obtained in Ref. [2]. The limit on the *LR* insertion parameter will become even stronger as the experimental limit on  $B_d \rightarrow X_d \gamma$  will be improved in the future.

In Fig. 2, we show the predictions for  $A_{ll}$  as a function of the KM angle  $\gamma$ : (a) *LL* insertion and (b) *LR* insertion only. For the *LL* insertion case [Fig. 2 (a)], one can expect a large deviation from the SM prediction for  $A_{ll}$  for a wide range of the KM angle  $\gamma$  ( $\sim -60^\circ \lesssim \gamma \lesssim +60^\circ$ ), even after we impose the  $B \rightarrow X_d \gamma$  branching ratio which is more constraining than the  $A_{ll}$  (the short dashed lines indicate the  $1\sigma$  range for  $A_{ll}^{\text{exp}}$ ). Also even if the KM angle  $\gamma$  is close to the SM value ( $\gamma \approx 55^\circ$ ), the dilepton charge asymmetry  $A_{ll}$  can be different from the SM prediction by a significant amount due to the SUSY contributions from  $(\delta_{13}^3)_{LL}$ . On the other hand, for the *LR* insertion case [Fig. 2 (b)], the  $B \rightarrow X_d \gamma$  constraint rules out essentially almost all the parameter space region, and the resulting  $A_{ll}$  is essentially the same as for the SM case.

In Figs. 3 (a) and (b), we show the branching ratio of  $B_d \rightarrow X_d \gamma$  and the direct CP asymmetry therein, respectively, as functions of the KM angles  $\gamma$  for the *LL* insertion only. The SM predictions

$$B(B_d \rightarrow X_d \gamma) = (0.9 - 1.1) \times 10^{-5}, \quad A_{CP}^{b \rightarrow d \gamma} = (-15 \sim -10)\%$$

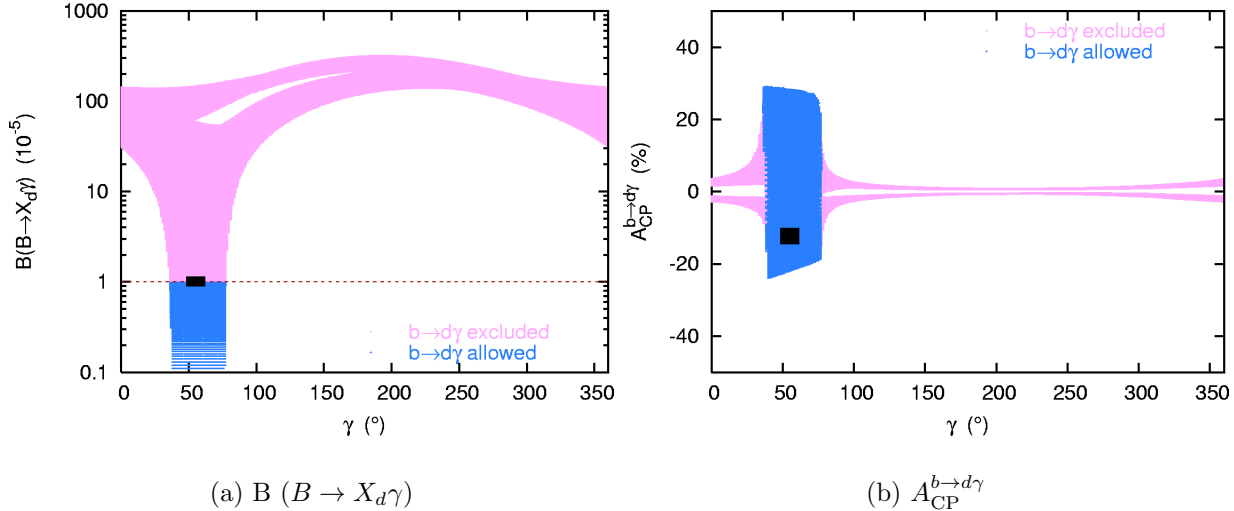


FIG. 4: The possible ranges of (a)  $B(B_d \rightarrow X_d \gamma)$  and (b)  $A_{CP}^{b \rightarrow d \gamma}$  as functions of the KM angle  $\gamma$  in the *LR* insertion case. The black rectangle around  $\gamma \simeq 55^\circ$  is the SM prediction. Those parameters which lead to  $B(B_d \rightarrow X_d \gamma) > 1 \times 10^{-5}$  are represented by the gray (magenta) region, and those for  $B(B_d \rightarrow X_d \gamma) < 1 \times 10^{-5}$  by the dark (blue) region.

are indicated by the black boxes. In this case, the KM angle  $\gamma$  is constrained in the range  $\sim -60^\circ$  and  $\sim +60^\circ$ . The direct CP asymmetry is predicted to be between  $\sim -15\%$  and  $\sim +20\%$ . In the *LL* mixing case, the SM gives the dominant contribution to  $B_d \rightarrow X_d \gamma$ , but the KM angle can be different from the SM case, because SUSY contributions to the  $B^0 - \bar{B}^0$  mixing can be significant and the preferred value of  $\gamma$  can change from the SM KM fitting. This is the same in the rare kaon decays and the results obtained in Ref. [15] apply without modifications. If the KM angle  $\gamma$  is substantially different from the SM value (say,  $\gamma = 0$ ), we could anticipate large deviations in the  $B_d \rightarrow X_d \gamma$  branching ratio and the direct CP violation thereof.

In Figs. 4 (a) and (b), we show the branching ratio of  $B_d \rightarrow X_d \gamma$  and the direct CP asymmetry therein, respectively, as functions of the KM angles  $\gamma$  for the *LR* insertion only. As before, the black boxes represent the SM predictions for  $B(B_d \rightarrow X_d \gamma)$  and the direct CP asymmetry therein. In the *LR* insertion case, there could be substantial deviations in both the branching ratio and the CP asymmetry from the SM predictions, even if the  $\Delta m_B$  and  $\sin 2\beta$  is the same as the SM predictions as well as the data. For the *LL* insertion, such a large deviation is possible, since the KM angle  $\gamma$  can be substantially different from the SM value. On the other hand, for the *LR* mixing, the large deviation comes from the complex  $(\delta_{13}^d)_{LR}$  even if the KM angle is set to the same value as in the SM. The size of  $(\delta_{13}^d)_{LR}$  is too small to affect the  $B^0 - \bar{B}^0$  mixing, but is still large enough to affect  $B \rightarrow X_d \gamma$ . Our model independent study indicates that the current data on the  $\Delta m_B$ ,  $\sin 2\beta$  and  $A_{ll}$  do still allow a possibility for large deviations in  $B \rightarrow X_d \gamma$ , both in the branching ratio and the direct CP asymmetry thereof. The latter variables are indispensable to test completely the KM paradigm for CP violation and get ideas on possible new physics with new flavor/CP violation in  $b \rightarrow d$  transition.

## IV. CONCLUSIONS

In this work, we considered the gluino-mediated SUSY contributions to  $B^0 - \overline{B^0}$  mixing,  $B \rightarrow J/\psi K_s$  and  $B \rightarrow X_d\gamma$  in the mass insertion approximation. We find that the (*LL*) mixing parameter can be as large as  $|(\delta_{13}^d)_{LL}| \lesssim 2 \times 10^{-1}$ , but the (*LR*) mixing is strongly constrained by the  $B \rightarrow X_d\gamma$  branching ratio:  $|(\delta_{13}^d)_{LR}| \lesssim 10^{-2}$ . The implications for the direct CP asymmetry in  $B \rightarrow X_d\gamma$  are also discussed, where substantial deviations from the SM predictions are possible both in the *LL* and *LR* insertion cases for different reasons. For the *LL* insertion case, the SUSY contribution to  $B \rightarrow X_d\gamma$  is not so significant, but is still constrained by the current upper limit on  $B \rightarrow X_d\gamma$ . (If the upper limit were  $B(B \rightarrow X_d\gamma) < 5 \times 10^{-5}$ , then the allowed region for the KM angle  $\gamma$  is the whole range from 0 to  $2\pi$ , as can be seen from Fig. 3 (a). In this case, the  $A_{ll}$  will provide a more important constraint for the *LL* insertion.) Also the global KM fitting can change because SUSY can affect  $B^0 - \overline{B^0}$  mixing by a significant manner. By the same reason, there is still ample room for large deviations in the  $A_{ll}$  for the *LL* insertion case. On the other hand, for the *LR* insertion case, the SUSY contribution to  $B \rightarrow X_d\gamma$  is enhanced by the factor  $m_{\tilde{g}}/m_b$  and the size of  $(\delta_{13}^d)_{LR}$  is strongly constrained. The resulting effect is that the KM angle cannot differ too much from the SM case. Still large deviations in the branching ratio for  $B \rightarrow X_d\gamma$  and direct CP violation thereof is possible due to large SUSY loop effects on  $B \rightarrow X_d\gamma$ . Thus it turns out that all the observables,  $A_{ll}$ , the branching ratio of  $B \rightarrow X_d\gamma$  and the direct CP violation thereof are very important, since they could provide informations on new flavor and CP violation from  $(\delta_{13}^d)_{LL,LR}$  (or any other new physics scenarios with new flavor/CP violations). Also they are indispensable in order that we can ultimately test the KM paradigm for CP violation in the SM.

### *Note Added*

While this work was being finished, we received a preprint [23], in which similar processes (the exclusive  $B \rightarrow \rho\gamma$  and various asymmetries thereof, and  $A_{ll}$ ) in certain class of SUSY models are considered.

### Acknowledgments

This work is supported in part by BK21 Haeksim program of the Ministry of Education (MOE), by the Korea Science and Engineering Foundation (KOSEF) through Center for High Energy Physics (CHEP) at Kyungpook National University, and by DFG-KOSEF Collaboration program (2000) under the contract 20005-111-02-2 (KOSEF) and 446 KOR-113/137/0-1 (DFG).

---

- [1] B. Aubert *et al.* [BABAR Collaboration], arXiv:hep-ex/0203007; T. Higuchi [Belle Collaboration], arXiv:hep-ex/0205020.
- [2] D. Becirevic *et al.*, arXiv:hep-ph/0112303.
- [3] D. E. Groom *et al.* [Particle Data Group Collaboration], Eur. Phys. J. C **15**, 1 (2000).
- [4] S. Laplace, Z. Ligeti, Y. Nir and G. Perez, Phys. Rev. D **65**, 094040 (2002) [arXiv:hep-ph/0202010].

- [5] A. Ali, G. F. Giudice and T. Mannel, Z. Phys. C **67**, 417 (1995) [arXiv:hep-ph/9408213]; Y. G. Kim, P. Ko and J. S. Lee, Nucl. Phys. B **544**, 64 (1999) [arXiv:hep-ph/9810336]; A. Ali, E. Lunghi, C. Greub and G. Hiller, arXiv:hep-ph/0112300.
- [6] F. Gabbiani and A. Masiero, Nucl. Phys. B **322** (1989) 235 ; J. S. Hagelin, S. Kelley and T. Tanaka, Nucl. Phys. B **415** (1994) 293 ; E. Gabrielli, A. Masiero and L. Silvestrini, Phys. Lett. B **374** (1996) 80 [arXiv:hep-ph/9509379]; F. Gabbiani, E. Gabrielli, A. Masiero and L. Silvestrini, Nucl. Phys. B **477** (1996) 321 [arXiv:hep-ph/9604387];
- [7] A. Ali and E. Lunghi, Eur. Phys. J. C **21**, 683 (2001) [arXiv:hep-ph/0105200]; A. Ali, Contribution to International Conference on Flavor Physics (ICFP 2001), Zhang-Jia-Jie City, Hunan, China, 31 May - 6 Jun 2001. arXiv:hep-ph/0201120.
- [8] L. Everett, G. L. Kane, S. Rigolin, L. T. Wang and T. T. Wang, JHEP **0201**, 022 (2002) [arXiv:hep-ph/0112126].
- [9] S. Baek and P. Ko, Phys. Rev. Lett. **83**, 488 (1999) [arXiv:hep-ph/9812229]; A. Ali and D. London, Eur. Phys. J. C **9**, 687 (1999) [arXiv:hep-ph/9903535]; A. Bartl, T. Gajdosik, E. Lunghi, A. Masiero, W. Porod, H. Stremnitzer and O. Vives, Phys. Rev. D **64**, 076009 (2001) [arXiv:hep-ph/0103324]; A. J. Buras and R. Fleischer, Phys. Rev. D **64**, 115010 (2001) [arXiv:hep-ph/0104238].
- [10] M. Convery [BABAR Collaboration], talk presented at the meeting of the APS Division of Particles and Fields DPF-2002, Williamsburg, Virginia, 24-28 May, 2002.
- [11] A. J. Buras, in 'Probing the Standard Model of Particle Interactions', F. David and R. Gupta, eds., 1998, Elsevier Science B.V. arXiv:hep-ph/9806471;
- [12] A. J. Buras, M. Jamin and P. H. Weisz, Nucl. Phys. B **347**, 491 (1990).
- [13] G. Buchalla, A. J. Buras and M. E. Lautenbacher, Rev. Mod. Phys. **68**, 1125 (1996) [arXiv:hep-ph/9512380].
- [14] D. Becirevic, V. Gimenez, G. Martinelli, M. Papinutto and J. Reyes, JHEP **0204**, 025 (2002) [arXiv:hep-lat/0110091].
- [15] S. Baek, J. H. Jang, P. Ko and J.H. Park, Nucl. Phys. B **609**, 442 (2001) [arXiv:hep-ph/0105028].
- [16] A. J. Buras and R. Fleischer, Adv. Ser. Direct. High Energy Phys. **15**, 65 (1998) [arXiv:hep-ph/9704376].
- [17] M. Ciuchini *et al.*, JHEP **0107**, 013 (2001) [arXiv:hep-ph/0012308].
- [18] L. Randall and S. Su, Nucl. Phys. B **540**, 37 (1999) [arXiv:hep-ph/9807377];
- [19] A. Ali, H. Asatrian and C. Greub, Phys. Lett. B **429**, 87 (1998) [arXiv:hep-ph/9803314].
- [20] A. L. Kagan and M. Neubert, Phys. Rev. D **58**, 094012 (1998) [arXiv:hep-ph/9803368].
- [21] A. G. Akeroyd, Y. Y. Keum and S. Recksiegel, Phys. Lett. B **507**, 252 (2001) [arXiv:hep-ph/0103008].
- [22] A. J. Buras, G. Colangelo, G. Isidori, A. Romanino and L. Silvestrini, Nucl. Phys. B **566**, 3 (2000) [arXiv:hep-ph/9908371]; T. Besmer, C. Greub and T. Hurth, Nucl. Phys. B **609**, 359 (2001) [arXiv:hep-ph/0105292];
- [23] A. Ali and E. Lunghi, arXiv:hep-ph/0206242.